Available online at www.sciencedirect.com
SCIENCE DIRECT
Journal of Power Sources 158 (2006) 446–454
JOURNAL OF POWER SOURCES
www.elsevier.com/locate/jpowsour

A polymer electrolyte fuel cell life test: 3 years of continuous operation

S.J.C. Cleghorn *, D.K. Mayfield, D.A. Moore, J.C. Moore, G. Rusch, T.W. Sherman, N.T. Sisofo, U. Beuscher

W.L. Gore & Associates, Inc., 201 Airport Road, P.O. Box 1488, Elkton, MD 21922, USA

Received 12 September 2005; accepted 19 September 2005
Available online 20 December 2005

Abstract

Implementation of polymer electrolyte fuel cells (PEMFCs) for stationary power applications requires the demonstration of reliable fuel cell stack life. One of the most critical components in the stack and that most likely to ultimately dictate stack life is the membrane electrode assembly (MEA). This publication reports the results of a 26,300 h single cell life test operated with a commercial MEA at conditions relevant to stationary fuel cell applications. In this experiment, the ultimate MEA life was dictated by failure of the membrane. In addition, the performance degradation rate of the cell was determined to be between 4 and 6 $\mu V\,h^{-1}$, at the operating current density of 800 mA cm^{-2}. AC impedance analysis and DC electrochemical tests (cyclic voltammetry and polarization curves) were performed as diagnostics during and on completion the test, to understand materials changes occurring during the test. Post mortem analyses of the fuel cell components were also performed.

Keywords: Polymer electrolyte fuel cells; Life test; Stationary fuel cells; Fuel cell diagnostics; AC impedance; Cyclic voltammetry

1. Introduction

Over the last decade, polymer electrolyte membrane fuel cells (PEMFCs) have received ever growing interest resulting in significant technological advancement, especially in areas of increasing power density and decreased materials utilization, with the advent of thin membranes [1] and reduced precious metal catalyst loadings [2]. PEMFCs have gained interest for many potential power source applications, including battery replacements for portable devices, automotive traction as replacement for the internal combustion engine and in stationary power generation. The cost targets and technology requirements facing the PEMFC seem exceedingly daunting to overcome before wide spread commercial automotive markets [3] are possible. As portable power sources fuel cells need to achieve higher power density to compete as battery replacements in the most attractive high-volume consumer markets (powering devices, such as cell phones, PDA and laptops) [4]. In contrast, it has been argued for many years that there may be fewer barriers to market entry for PEMFCs as stationary power plants [5]. For this application, systems cost targets are much less demanding than automotive, fuel is widely available (storage and infrastructure are not a problem) and typically volumetric and gravimetric constraints are not critical, allowing the fuel cell to be operated at favorable conditions.

Stationary fuel cell power plants are attractive, as they offer the potential of higher efficiency and lower greenhouse gas emissions, than available technologies and may be cost-competitive with grid power in areas where the cost of electricity is expensive relative to natural gas. Alternatively, fuel cells may be preferred where grid connection is not practical or does not offer reliable power.

The key to the commercial implementation of stationary fuel cell systems is the demonstration of reliable long life. In fact, it is generally recognized that a cost-effective stationary fuel cell power plant requires the fuel cell stack life expectancy to exceed 40,000 h. The critical component of the fuel cell, and the component that is most likely to dictate stack life, is the membrane electrode assembly (MEA). Until very recently, there was very little publicly available data demonstrating extended

* Corresponding author. Tel.: +1 410 506 7634; fax: +1 410 506 7633.
E-mail address: scleghorn@wlgore.com (S.J.C. Cleghorn).

0378-7753/$ – see front matter © 2005 Elsevier B.V. All rights reserved.
doi:10.1016/j.jpowsour.2005.09.062

operational life of PEMFCs, and also few publications reporting the mechanisms of MEA performance loss and failure after extended operation. This is probably because much of this activity has been confined to the industrial sector. However, in recent years, there has been a significant increase in publicly available data, as a result of increasing academic activity and an increasing willingness of industrial organization to publish. Several recent reviews have compiled many of the literature publications referencing PEMFC durability [6], and ionomer membrane degradation [7].

The longest PEMFC demonstration that we are aware of in the open literature was a 60,000 h life test reported by GE in 1979 [7–9]. This GE stack module was operated with pressurized hydrogen/oxygen and used MEAs based on NAFION® 120 membrane (250 μm thick). The limited post mortem data reported from this test demonstrated the tensile properties of the membranes had deteriorated, while the BET surface area of the catalyst was not changed. St-Pierre and Jia [10] more recently reported extended operation for a hydrogen/oxygen stack, with a voltage decay rate of less than $2\,\mu V\,h^{-1}$ in 11,000 h of operation without failure. Kinetic, ohmic and transport losses in the stack over its life were monitored. The diagnostics and post mortem analysis reported the primary cause for power loss was increased mass transport over-potential, this was attributed to an increased hydrophilicity of the gas diffusion media.

Within the last several years there has been a proliferation of publications reporting several thousands of hours of single cell and short stack life, presumably using much thinner membranes and lower catalyst loadings (the MEA characteristics are not always disclosed) than the early GE stack. Several notable examples include single cell demonstrations performed at Osaka gas [11], some of which have exceed 17,000 h life with voltage decay rates of less than $5\,\mu V\,h^{-1}$, operating with reformate fuel [12,13]. Fuji Electric Co. Ltd. reported 10,000 h of hydrogen operation [14] in a single cell and reported over 15,000 h, with no significant voltage decay at $0.4\,A\,cm^{-2}$ for a 45-cell stack. In addition, Wilkinson and St-Pierre of Ballard [6] have published results of a series-of-life tests operated with reformate fuel in short stacks, the longest of which has exceeded 13,000 h without failure, with a reported voltage decay rate of $0.5\,\mu V\,h^{-1}$ [15].

There is also a growing body of literature outlining various in situ electrochemical methods [16,17] and ex situ analytical techniques [18–21], which can be employed to characterize MEAs either during life testing or upon failure, to understand MEA and fuel cell degradation mechanisms. However, there are very few examples of publications that deploy the known analytical techniques to understanding changes occurring in the MEA during extended life testing. In this publication, we report results of what we believe to be the longest single cell fuel cell life test operated with a commercial MEA and the associated diagnostic results which were used to understand materials changes occurring during the test. This MEA has both membrane thickness and precious metal loading consistent with meeting the cost targets for stationary fuel cell applications.

2. Experimental

This publication focuses on the results obtained from the operation of a single cell PEMFC life test, which was operated under continuous load for 3 years (over 26,000 h), the diagnostics performed during the course of the life test, and the post mortem analysis performed on the components on completion of the test.

The life test was performed in 25-cm^2 single cell hardware (Fuel Cell Technologies, Albuquerque, NM). Anode and cathode flow fields, were both triple channel serpentine designs machined into graphite (POCCO graphite) and were assembled in co-flow orientation. The cell was assembled with a Gore PRIMEA® Series 5621 MEA; based on a 35 μm GORE-SELECT® membrane with a cathode loading of $0.6\,mg_{Pt}\,cm^{-2}$ and an anode with Pt–Ru alloy loading of $0.45\,mg\,cm^{-2}$. Gore CARBEL™ CL gas diffusion media was used on both anode and cathode sides of the cell[1]. An incompressible silicone coated fiberglass gasket (CHR–furon) was used on either side of the membrane to provide cell sealing. A second thin incompressible gasket, referred to as a sub-gasket, was placed between the MEA and gas diffusion media to define the cell active area of 23 cm^2. The gasket arrangement was chosen and cell assembly was performed such that the average active area compression was approximately 150 psi (the assembly pressure was predetermined using PRESSSUREX pressure sensitive paper from Sensor Products, Inc., NJ). The eight lubricated bolts of the cell hardware were torqued to 45 in lbs per bolt.

Reactant humidification, gas flow rate, back-pressure and cell temperature were all controlled from a fuel cell test station (Globetec, now Electrochem, Boston, MA). During the 3 years of continuous operation of the life test, the cell temperature was controlled at 70 °C, the outlet reactant pressures were maintained at ambient pressure, reactants were stoichiometrically controlled and the reactants were saturated at cell temperature. It is very important to highlight that significant effort was given to controlling the reactant inlet relative humidity to 100% RH. To prevent liquid water from entering the fuel cell, liquid water traps were used and the reactant gas lines into the fuel cell were heated a few degrees above the cell temperature. Several times during the experiment the test was stopped and the test station re-calibrated. Current, voltage and cell resistance (by current interrupt) data were collected as a function of time, over the entire length of the test using a computer controlled Scribner electronic load (Scribner and Associates, Southern Pines, NC).

Much of the first 3000 h of this life test were performed with a simulated reformate fuel of composition: 43% nitrogen, 17% carbon dioxide, 50 ppm carbon monoxide and a balance of hydrogen. In addition 4% air bleed was used to mitigate the effects of CO poisoning. The detailed description of this data is the subject of another publication [22]. However, the remaining 23,000 h, and therefore the majority of this life test, was performed with pure hydrogen fuel (99.999% hydrogen). Filtered, compressed and dried air was used throughout the test.

[1] GORE, CARBEL, GORE-SELECT, PRIMEA and designs are trademarks of W.L. Gore & Associates, Inc.

The life test was operated continuously at constant current of 800 mA cm^{-2}. The life test was interrupted approximately every 500 h to perform in-cell electrochemical diagnostics in a systematic manner. To interrupt the test, the load was disconnected and reactant flows stopped. The cathode compartment of the fuel cell was switched to fully humidified nitrogen flow. Once the open cell voltage (OCV) had reached a steady-state value of less than 100 mV, cyclic voltammetry and electrochemical hydrogen cross-over measurements were performed on the cell. Once these diagnostics had been completed the cell was returned to the hydrogen/air life test operation at constant current, 800 mA cm^{-2}. After several hours operation, a polarization curve was performed under voltage control. Upon completion of the life test, more extensive in-cell diagnostics (AC impedance [23]) and out-of-cell diagnostics were performed to try to further elucidate material changes that may have occurred during the extended operation of this fuel cell.

In order to understand MEA integrity and performance decay in operating fuel cells, we have found it extremely valuable to identify and define the following terms [24]:

2.1. Reliability

MEA reliability failure is typically defined as either inability of the MEA to operate in a stack or single cell at start-up, or a short-term (less than 100 h) membrane failure. MEA reliability may be associated with the use of defective MEAs, or the result of poor cell or stack design or assembly, causing MEA shorting, puncturing or "burn-through". MEA reliability problems are addressed with attention to MEA manufacturing quality, proper handling, and effective cell or stack design, and are not the discussed in this publication.

2.2. Durability

The overall cell performance decay rates, measured during continuous and uninterrupted operation, is the sum of both stability and durability decay rates. The durability decay rate is defined as the unrecoverable portion of this total decay rate. This is measured from comparing cell performances in polarization curves as a function of time (or comparing cell performance after recovery techniques). Durability decay rate is a result of irreversible materials changes occurring in the cell (i.e. loss in electrochemical surface area or carbon corrosion, etc.).

2.3. Stability

The stability decay rate is the recoverable function of the power loss observed during continuous operation. The stability decay rate is calculated by subtracting the durability decay rate (i.e. the portion that was not recovered from performing polarization curves) from the total decay rate. MEA performance lost as a result of stability decay is typically concerned with non-steady-state behavior and is associated with sensitivity to operating conditions (water management) and reversible materials changes.

3. Results and discussion

3.1. Life test operation

The cell voltage, *iR* compensated cell voltage and cell resistance for the entire 26,300 h life test as a function of time on load operated at constant current, 800 mA cm^{-2} are shown in Fig. 1. The initial performance of this cell operated on hydrogen was 0.65 V at 800 mA cm^{-2}, upon completion of the test the performance had declined to approximately 0.54 V. This is a total voltage loss of 110 mV in 26,300 h and corresponds to an overall voltage decay rate of 4.2×10^{-6} V h^{-1} (or 4.2 μV h^{-1}). A linear regression fitted through the voltage data at 800 mA cm^{-2} for the hydrogen fueled operating period of the experiment (from 3000 to 26,300 h) produced an overall voltage decay rate of 6.4 μV h^{-1}. Both of these overall decay rates are examples of what we have defined as a durability decay rate, as the cell performance was periodically recovered by performing in-cell diagnostics (discussed below).

It can also be ascertained from Fig. 1 that the measured resistance for the cell is observed to undergo very little overall change during the life of the test, actually decreasing from approximately 82 mΩ cm^2 to approximately 68 mΩ cm^2 in 26,300 h.

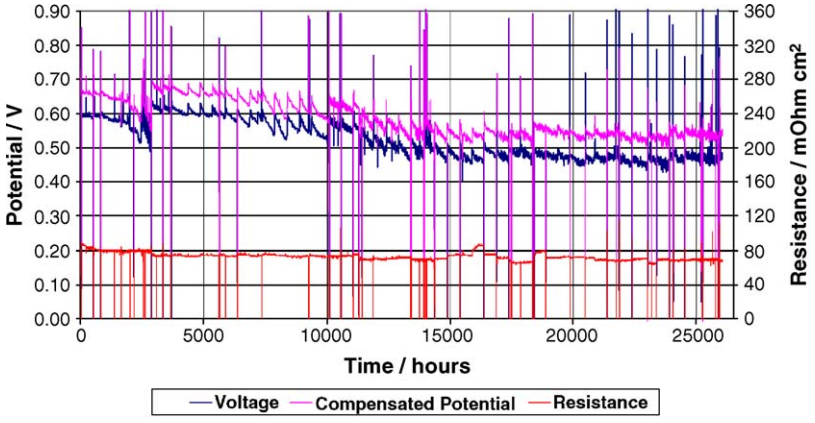

Fig. 1. Cell voltage, *iR* compensated cell voltage and cell resistance as a function of hours on load operated at constant current, 800 mA cm^{-2} for the entire 26,300 h life test. Cell temperature 70 °C. Air: 2.0× stoichiometry, ambient pressure, 100% RH. Hydrogen: 1.2× stoichiometry, ambient pressure and 100% RH.

This change is expected to result in an 11 mV increase in performance at 800 mA cm^{-2}. It is, therefore, evident that the source of voltage decay apparent in the test cannot be accounted for by an increase in membrane resistance. This is confirmed by the *iR* corrected voltage decay rate matching the decay rate of the raw voltage data (also shown in Fig. 1).

One characteristic of this test, worth further comment, is the saw-tooth behavior of the voltage trace over the length of the life test, with a typical periodicity of approximately 500 h. The peak in the saw-tooth co-insides with re-starting of the test following interruption to perform fuel cell diagnostics. This result demonstrates that interruption of the life test and performance of electrochemical diagnostics provides recovery of the cell voltage. The cell voltage again typically decays upon re-starting the fuel cell under load after completion of diagnostics. To illustrate the effect of the diagnostics typical detailed voltage/time plots at two different periods in time are shown in Fig. 2a and b. The examples demonstrate that interruption of the test to perform diagnostics recovered cell performance by approximately 80 mV (Fig. 2a, from 7300 to 9000 h) and approximately 40 mV (Fig. 2b, from 20,300 to 21,700 h). This corresponds to stability decay rates of approximately 140 and 40 μV h^{-1}, respectively. It is believed that MEA performance decay, resulting from cell instability, was typically the result of non-steady-state behavior, and therefore by definition, was fully recoverable. MEA stability is associated with the MEA's sensitivity to operating conditions (i.e. water management) or reversible material changes (such as formation of formation of Pt oxides, adsorption of poisons or an increase in oxygen transport resistance as a result of formation of liquid water barriers). The stability decay rate between recoveries can be quite variable, and is also relatively high, compared to the reported durability decay rate. The data plotted in Fig. 2a and b also indicates that although there is a concurrent saw-tooth behavior in the measured cell resistance, it cannot account for the magnitude of the voltage changes observed.

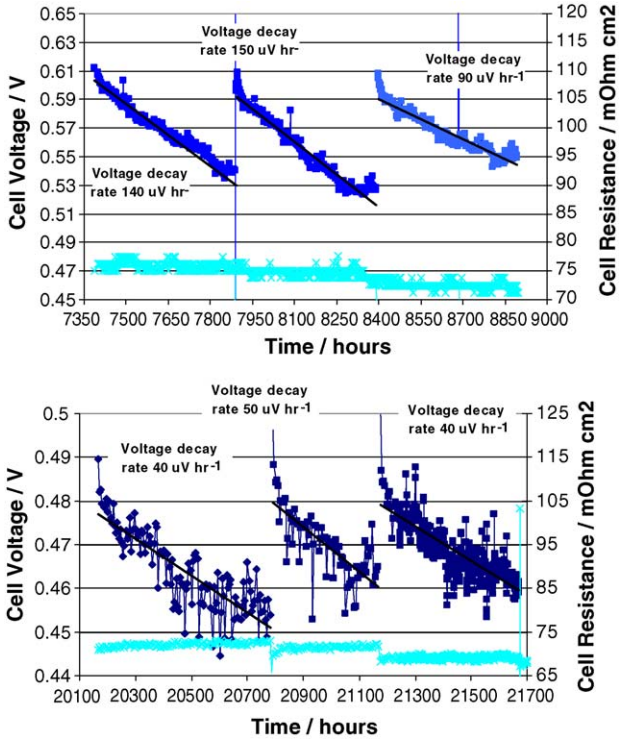

Fig. 2. Detail of cell voltage and cell resistance as a function of time on load operated at constant current of 800 mA cm^{-2} for (a) 7390–8890 h and (b) 20,170–21,670 h. Cell temperature 70 °C. Air: 2.0× stoichiometry, ambient pressure, 100% RH. Hydrogen: 1.2× stoichiometry, ambient pressure and 100% RH.

3.2. In fuel cell diagnostics

There is always a trade-off when designing fuel cell life test experiments as to the value of operating the test with or without interruption to perform diagnostic experiments. Of course operation without periodic diagnostics is more likely to approach cell operation in the application. However, when starting this experiment, there were very few publications reporting the effects of long-term operation on the materials within the cell. Therefore, it was our philosophy in this life test to perform diagnostics in order to maximize our learning from this experiment.

3.2.1. Cyclic voltammetry

The life test was interrupted every 500 h (later in the test, the uninterrupted period of operation was increased to every 1000 h) of load operation to perform diagnostics. First cyclic voltammetry was performed with the fuel cell cathode as the working electrode. Three complete voltage scans from 10 to 1200 mV (using the hydrogen electrode as the counter and reference) were recorded at 100 mV s^{-1}, the results of the third scan at various selected periods in time are compiled in Fig. 3. The voltammetry scan at 0 h was typical of those recorded for fuel cell electrodes, and the description of the various peaks is reported elsewhere in the literature [16]. As the life test progressed, the charge associated with platinum oxide formation and reduction, was observed to decrease, while the double layer capacitance charge shows a slight increase. It is also important to comment that there is no evidence for additional or unexpected peaks developing in the

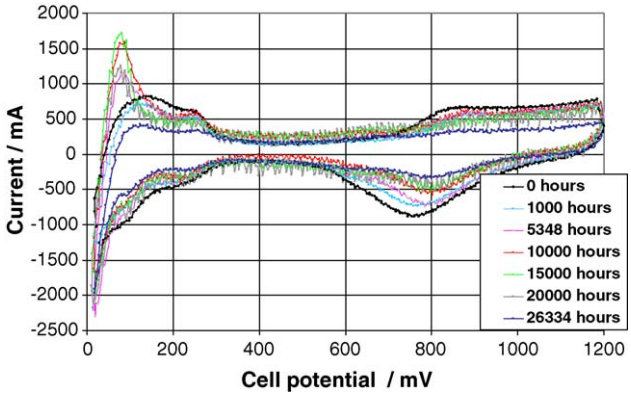

Fig. 3. Cyclic voltammetry recorded at 0, 1000, 5348, 10,000, 15,000, 20,000 and 26,334 h during the life test. Voltage scan between limits 10 and 1200 mV at a potential scan rate of 100 mV s^{-1}. Cell temperature 70 °C. Working electrode (fuel cell cathode) 50 ml min^{-1} nitrogen, ambient pressure and 100% RH. Secondary and reference electrode (fuel cell anode): 50 ml min^{-1} hydrogen, ambient pressure, 100% RH.

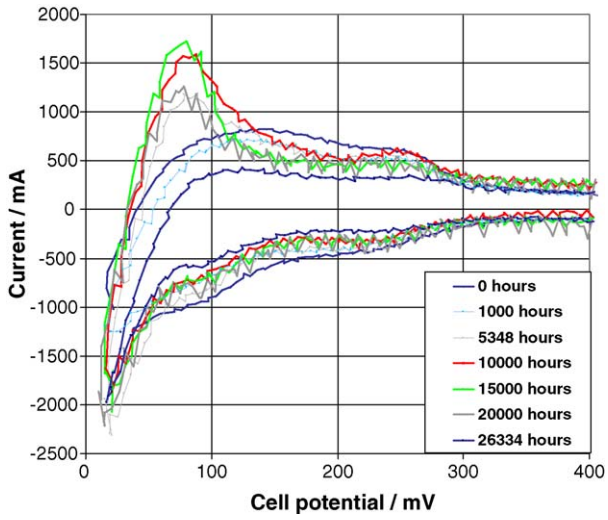

Fig. 4. Detail of cyclic voltammetry in the hydrogen region during the life test (see Fig. 5 for details).

voltammetry during the test, which might indicate the introduction of adsorbed electro-active poisons at the cathode electrode. The primary motive for performing cyclic voltammetry during this life test was to quantitatively monitor the change in electrochemically active area (ECA) of the cathode, by measuring the charge associated with hydrogen adsorption and desorption (Fig. 4). In our experiments at Gore, we have been much more successful at quantifying ECA from the hydrogen oxidation peaks of the voltammetry (compared to hydrogen desorption). In this experiment, the apparent charge associated with the hydrogen oxidation region does not significantly change throughout the 26,300 h life test (Fig. 5, total hydrogen oxidation charge). However, further analysis of the data indicates that a large oxidation peak developed at 80 mV (see scans at 5000, 10,000, 15,000 and 20,000 h in Fig. 4). This peak, at approximately 80 mV, is likely to be associated with oxidation of molecular hydrogen, formed on the reverse scan in the voltamogram. By curve fitting, the charge for molecular hydrogen oxidation was estimated in each voltammogram, and then subtracted from the total charge measured in the hydrogen region. Fig. 5 shows the total charge measured in the hydrogen region, the estimated charge associated with molecular hydrogen oxidation and the charge calculated for oxidation of adsorbed hydrogen (or ECA) as a function of time. As commented before, the total hydrogen oxidation charge does not change significantly within the test. Interestingly, the fitted molecular hydrogen oxidation charge appears to increase to a maximum at approximately 15,000 h, after which the data becomes quite noisy. Despite this noise in the data, the calculated ECA consistently decreases throughout the life test. In total, it was estimated that approximately 66% of ECA was lost in 26,300 h of operation. Linear interpolation of the data gave a reasonably good fit, with a loss of ECA of 1×10^{-6} C cm^{-2} h^{-1}. Using a simple Tafel kinetic calculation and assuming a Tafel slope of 70 mV per decade [25], it can be calculated that a 66% loss in ECA should result in a 34 mV loss in cell performance.

We have not been able to adequately understand the reason for the erratic behavior in formation of molecular hydrogen during this test, however, it does suggest that the working electrode was allowed to proceed to a lower potential than desirable for the ECA measurement. Two possible explanations for molecular hydrogen formation could be: (a) a shift in the reference electrode potential or (b) a change in the catalytic nature of the working electrode. It is unlikely that cell resistance change is responsible for this behavior. It was decided that we should maintain the starting potential at 10 mV, during the length of this experiment, and use regression methods to eliminate the additional charge resulting from molecular hydrogen oxidation in determination of the ECA.

3.2.2. Hydrogen cross-over

A key MEA characteristic, measured throughout the life test, was hydrogen cross-over through the ionomer membrane, which provides data on the health of the membrane. This was measured by the electrochemical technique [26], each time the cell was interrupted for diagnostics. A membrane is determined to have failed when the hydrogen cross-over current density exceeds between 10 and 15 mA cm^{-2}. (This is an arbitrary value used to provide a consistent end point to life tests, even though at this hydrogen permeation rate, no impact on cell performance is observed.) The initial (0 h) hydrogen cross-over current density was less than 1 mA cm^{-2}, no measurable change in hydrogen

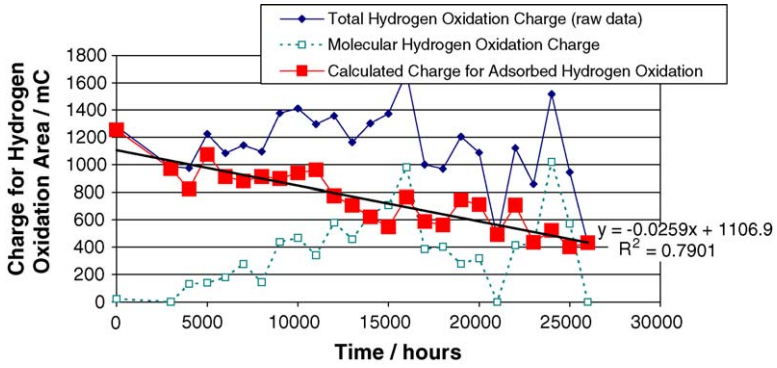

Fig. 5. Analysis of charge measured in the hydrogen oxidation region during the cyclic voltammetry experiments as a function of time over the peroid of the life test. Molecular hydrogen oxidation was estimated from curve fitting the voltammetric peak at 80 mV. The charge for adsorbed hydrogen (used for ECA) is calculated from total charge minus charge for molecular hydrogen oxidation.

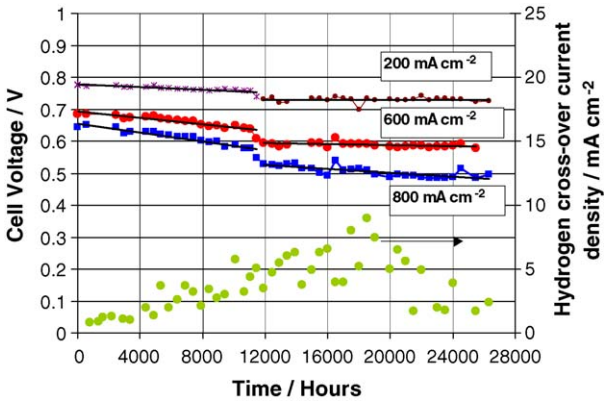

Fig. 6. Cell voltage interpolated from polarization curves at 200, 600 and 800 mA cm^{-2} and hydrogen cross-over current density as a function of time measured during the life test. Cell temperature 70 °C. Air: 2.0× stoichiometry, ambient pressure, 100% RH. Hydrogen: 1.2× stoichiometry, ambient pressure and 100% RH.

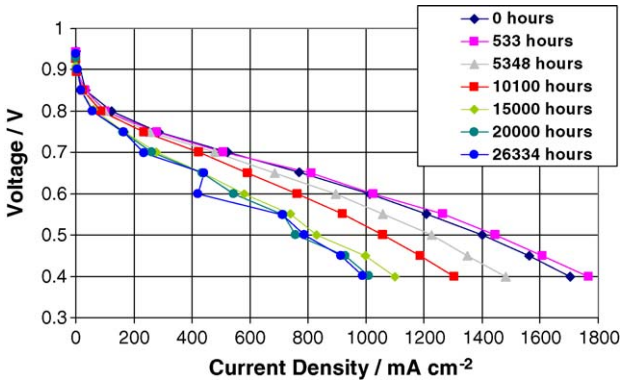

Fig. 7. Polarization curves at various periods in time (0, 500, 5348, 10,100, 15,000, 20,000 and 26,330 h) during the life test. Cell temperature 70 °C. Air: 2.0× stoichiometry, ambient pressure, 100% RH. Hydrogen: 1.2× stoichiometry, ambient pressure and 100% RH.

cross-over current was apparent until at least 5000–7000 h of operation (Fig. 6). After approximately 1 year of operation, the hydrogen cross-over current density follows a slow increase to approximately 22,000 h. This data can be reasonably fitted to an exponential curve, $y = 1.33\exp(8 \times 10^{-5}t)$. After 22,000 h operation, the measured hydrogen cross-over current density was observed to decrease to approximately 2–3 mA cm^{-2}. This effect was extensively investigated at the time, by varying the hydrogen overpressures, and measuring hydrogen cross-over current density cathode to anode and vice-versa. The data was found to be repeatable (Fig. 6 from 22,000 to 26,000 h). The reason for the change in behavior of the cell to the electrochemical test is not fully understood, however, it should also be pointed out that this is the first life test exceeding 20,000 h that we are aware of that has been monitored in this manner. When observing this apparently unreliable electrochemical data, a physical method of measuring hydrogen gas flow rate through the membrane using a bubble flow meter, was added to our diagnostics for this life test. At approximately 26,000 h, the life test was reported as failed when the volumetric flow rate of hydrogen through the membrane exceeded a value corresponding to 10 mA cm^{-2} equivalent hydrogen cross-over current density. It is also of interest to comment that extrapolating the exponential fit for the hydrogen cross-over data determined electrochemically (0–22,000 h) predicted a membrane life of 25,200 h.

The electrical short resistance through the membrane was also monitored throughout this life test, by calculating the slope of the limiting current density plateau, measured in hydrogen cross-over experiment. The data showed no trend over time and there was no evidence that electronic shorting was a concern in this test.

3.2.3. Polarization curves

Probably the most ubiquitous diagnostic performed in PEMFCs is the polarization curve. Fig. 7 shows a sample of polarization curves recorded under potential control, at various times throughout the life test, on completion of the voltammetric experiments. The data demonstrates loss in fuel cell performance throughout the polarization curve, without any significant change in the overall characteristics of the curve.

The cell voltage, as a function of time at 200, 600 and 800 mA cm^{-2}, has been determined by interpolation of the polarization curves. A linear curve fit through this data was used as a further method to determine the voltage decay rate for the life test (Fig. 6). This is also considered to be durability decay rate. The calculated decay rates are reported in Table 1. As well as reporting an overall decay rate for the entire test at each current density, decay rates have also been calculated for the time period 0–12,000 h and from 12,000 to 26,300 h. There is an easily identifiable step in the data at 12,000 h. This is much more difficult to identify in the raw data (Fig. 1). At approximately 11,500 h, the cell was maintained under load with much reduced air feed for approximately 24 h. This caused the cell voltage to be reduced to approximately 0 V while the cell operated at 1× stoichiometric air flow. (It was postulated that this condition may have results in localized hydrogen evolution at the cathode.) This error in operation resulted in a 20–30 mV performance loss at 800 mA cm^{-2} which was not recovered throughout the remainder of the life test.

Table 1
Voltage decay rates for the life test as a function of current density

Current density (mA cm^{-2})	Decay rate 0–12,000 h (μV h^{-1})	Decay rate 12,000–26,300 h (μV h^{-1})	Overall decay rate (μV h^{-1})
200	2	0.7	2
600	5	0.8	5
800	7	3	7

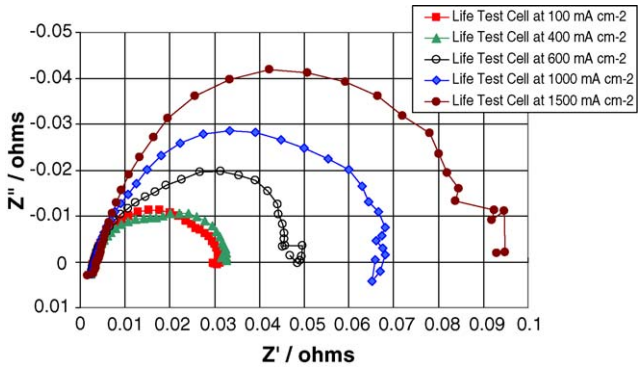

Fig. 8. Nyquist plot for the life-tested cell at the end of life (26,300 h) as a function of current density. Cell temperature 70 °C. Air: 2.0× stoichiometry, ambient pressure, 100% RH. Hydrogen: 1.2× stoichiometry, ambient pressure and 100% RH.

3.2.4. AC impedance

AC impedance was only performed on the life-tested cell on completion of the test after 26,300 h of operation. The impedance scans for fuel cell operated at a variety of current densities are shown from 8 kHz to 0.1 Hz (Fig. 8). This data has been compared to AC impedance data collected after break-in for a fuel cell built with the same hardware, as used in the life test, assembled with a new MEA from an identical lot as used in the life test (Fig. 9). The high-frequency resistance measured for the life-tested cell is approximately 75 mΩ cm^2 (at 1500 mA cm^{-2} the high-frequency resistance is increased to 85 mΩ cm^2). This resistance measured by impedance agrees very well with the cell resistance data measured by current interrupt shown in Fig. 1. The new cell has a slightly higher high-frequency resistance (between 94 and 99 mΩ cm^2), which is not significantly increased at 1500 mA cm^{-2}.

Considering the entire frequency scan at low current density (100 mA cm^{-2}), the impedance for the life tested and new cells appears very similar, with similar total impedance. It is expected that electron transfer resistance should dominate the impedance characteristic of the cell at this current density, and it is, therefore, implied that the electron transfer (or kinetic) resistance of the life-tested cell is not significantly changed. This may be a surprising result, considering the large change in ECA measured in voltammetry. At moderate current density (600 mA cm^{-2}), where fuel cell processes are expected to be under mixed kinetic and diffusion control, and high-current density (1500 mA cm^{-2}), where diffusion processes should be in control, the new and life-tested cells demonstrate very different behavior. In these current density ranges, the total impedance of the life-tested cell is dramatically increased relative to the new cell. This data suggests that the resistance to transport, or diffusion processes, has significantly increased between the new cell and the life-tested cell. In fact, even at 600 mA cm^{-2} where the new cell shows features of both kinetic and transport resistance, the life-tested cell impedance is dominated by transport resistance. To understand the source of the increased transport resistance AC, measurements of the life-tested cell were recorded when the reactant RH was reduced. At 1500 mA cm^{-2}, this resulted in a significant reduction in the total impedance (430 mΩ) of the cell. This observation might be consistent with the presence of liquid water impeding transport of reactant gases to active catalyst sites.

AC impedance can also be a valuable tool, in the absence of faradic reactions, to elucidate any change in the ionic conductivity of the electrodes, which may provide evidence for changes in ionomer structure or ionomer degradation in the electrode layer. Fig. 10 shows the impedance spectra for the life-tested cell between 0.1 Hz to 20 kHz at 80 °C with nitrogen flowing on both sides of the cell at four different relative humidities. Impedance spectra using this technique have been previously described [23]. At higher frequencies the Nyquist plot shows a 45° slope characteristic of proton transport in the catalyst layer. Then an infection in the curve occurs at lower frequency where the impedance becomes dominated by the electrode capacitance. We have defined this inflection as $R_i/3$, where R_i is the ionic resistance of the catalyst layer. The raw data demonstrates that the impedance of the electrode layer increases with decreased relative humidity. It is also evident that at lower frequency there

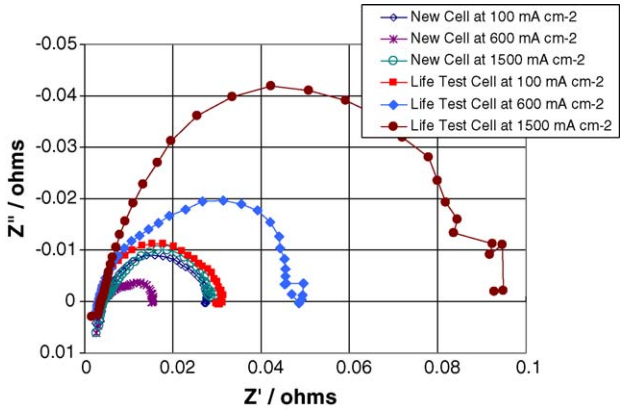

Fig. 9. Nyquist plot comparing the life-tested cell at the end of life (26,300 h) and a new cell at 100, 600 and 1500 mA cm^{-2}. Cell temperature 70 °C. Air: 2.0× stoichiometry, ambient pressure, 100% RH. Hydrogen: 1.2× stoichiometry, ambient pressure and 100% RH.

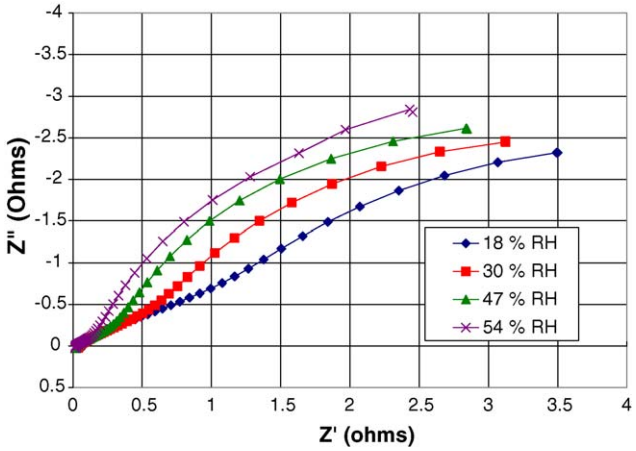

Fig. 10. Nyquist plot for the life-tested cell at the end of life (26,300 h) as a function of cell relative humidity (18, 30, 47 and 54%) in the presence of an inert gas. Cell temperature 70 °C. Nitrogen (provided to both cell compartments): flow rate 50 ml min^{-1}, ambient pressure.

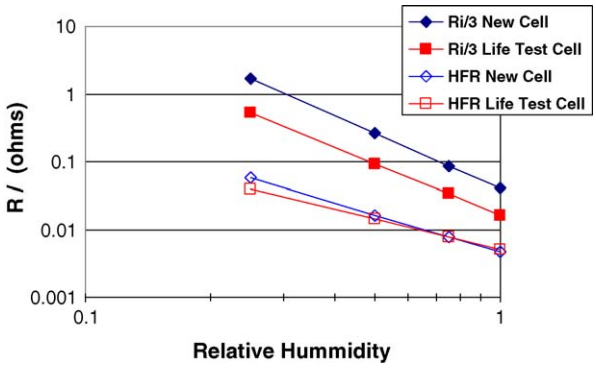

Fig. 11. High-frequency resistance (HFR) and ionic resistance of the electrode (R_i/3) as a function of relative humidity for the life-tested cell at the end of life (26,300 h) and a new cell. Cell temperature 70 °C. Nitrogen (provided two both cell compartments): flow rate 50 ml min^{-1}, ambient pressure.

is a large deviation from the vertical behavior expected for a capacitive electrode. This data suggests there is some evidence of electric shorting in the cell at the reduced relative humidity in which these measurements were performed. (The DC measurements at fully saturated conditions did not indicate presence of electrical shorts.)

Again we have compared the impedance data collected in this experiment, with a new cell after break-in, as a function of RH (Fig. 11). Once again it was concluded that there is no appreciable difference in the HFR of the new and life-tested cells. There is, however, a difference in the electrode impedance between the new and used cells; the ionic resistance in the catalyst layer is determined to be significantly reduced in the life-tested MEA when compared to the new MEA. We have observed this behavior in a number of our life-tests and have several hypothesis which can account for this behavior. (1) Over the life of the test, ionic pathways in the electrode are improved compared to a new MEA (consider MEA break-in). (2) During the life-test, ionic conduction pathways have been cut as a result of ionomer degradation: the impedance technique is now only able to access to a reduced depth in the electrode, because a smaller fraction of the electrode is now accessible the apparent ionic resistance of the electrode layer is decreased.

3.3. Post mortem analysis

At 26,300 h the life test was concluded as a result of the hydrogen gas cross-over exceeding our pre-determined criteria for failure. Upon conclusion of the life test, the cell was disassembled and components analyzed.

3.3.1. Gasket

On disassembly of the cell, the only visual change in the cell was the apparent degradation of the silicone/glass re-enforced gasket. Upon measurement, the gasket thickness was typically reduced by approximately 25 μm. This silicone degradation was so severe at active area edges, that in these areas only the glass re-enforcement remained. Silicone particles from the gasket were also observed on the surface of the gas diffusion media. We have concluded that the gasket changes observed were the cause for the cell to loss compression during the test (the cell was re-torqued on several occasions). Gasket degradation may have several effects on fuel cell performance in this life test: (i) increase the load on the gas diffusion media, leading to decreased porosity and increase reactant transport resistance; (ii) increase hydrophilicity of the gas diffusion media; (iii) poisoning of the catalysts.

3.3.2. Gas diffusion media

On completion of the test, the CARBEL® CL gas diffusion media on both sides of the membrane were strongly adhered to the electrodes of the MEA. The gas diffusion layers were removed from the MEA, however, the micro-layer remained stuck to the electrodes. Because the electrochemical data suggests that the mass transport resistance of the cell was increase over the life of the test, we were interested to determine whether any change in the gas diffusion media could be observed. It has been observed in our lab and others [10] that the after life testing some gas diffusion media types will pick-up water when immersed in boiling water. On completion of the life test, both anode and cathode gas diffusion media were immersed in water at 80 °C for over 500 h, no observable water pick-up was observed for these materials, indicating no change in the material could be detected by this test. SEM of the gas diffusion media, after testing, also indicated no observable change.

3.3.3. Membrane electrode assembly

SEM analysis of the failed MEA was focused on two areas, the reactant inlet area and an edge area close to the reactant exits. The most obvious observation through both of these areas was the wide spread presence of silicon contamination, which was confirmed by EDS mapping. The silicon found in the MEA, at the end of the life test, was thought to have been introduced by degradation of the silicone gaskets that were used in this test. The presence of significant quantities of silicon made the SEM cross-sections very difficult to interpret; however, it was evident that severe membrane thinning had occurred and was observed in both areas of the MEA that were sectioned. It was found that ionomer loss was most severe at the cathode side of the membrane, although ionomer loss from the anode side was also observed. The cross-sectional analysis demonstrated no observable change in the electrodes: no electrode thinning was observed on either anode or cathode electrodes, which suggests that there was no evidence of carbon corrosion. The back-scatter electron images showed no evidence of platinum rearrangement in the electrode or dissolution of platinum into the membrane. Further EDS analysis provided no evidence of ruthenium migration to the cathode.

4. Conclusions

In this publication we have reported the results of a 26,300 h life-test, performed in single cell hardware, at test conditions relevant to a stationary fuel cell application. The fuel cell life was limited in this test by the failure of the membrane, due to increased hydrogen gas cross-over. In this experiment, the cell performance degraded at a rate of between 4 and 6 × 10^{-6} V h^{-1}

at the operating current density of 800 mA cm^{-2}, corresponding to a maximum total voltage loss of less than 150 mV over the length of the test. The diagnostic experiments performed, during and on completion of the test, indicate that approximately 66% of the original cathode electrochemical area was lost. It was estimated that this loss in electrocatalytic surface area might only account for about 34 mV of the total cell performance loss. It was concluded from the AC impedance analysis that the major contribution to cell performance loss was due to increased transport losses in the cell. We have been unable to completely explain the source of this increase in transport resistance from the experiments that were performed, however, we suspect that the detected presence of silicone contamination may have strongly influenced the performance of the cell.

Acknowledgements

The authors would like to acknowledge the contribution of the entire W.L. Gore and Associates, Inc., Gore Fuel Cell Technologies team for their support of this test over the 3 years life of this experiment, especially the team dedicated to understanding MEA durability, which includes Dan Frydrych, Wen Liu and Mahesh Murthy. The authors are also grateful for the SEM analysis performed by Judy Rudolph.

References

[1] J.A. Kolde, B. Bahar, M.S. Wilson, T.A. Zawodzinski, S. Gottesfeld, Proton Conducting Membrane Fuel Cells, PV95-23, Electrochemical Society, Pennington, NJ, 1995.
[2] M.S. Wilson, S. Gottesfeld, J. Appl. Electrochem. 22 (1992) 1.
[3] M. Mathias, H.A. Gasteiger, Electrochemical Society Proceedings, vol. PV 2002-31, in: M. Murthy, T.F. Fuller, J.W. Van Zee, S. Gottesfeld (Eds.), Third International Symposium on PEM Fuel Cells, Salt Lake City, UT, 2002.
[4] D. Jollie, Fuel Cell Market Survey: Portable Applications, www.fuelcelltoday.com, 6 September 2005.
[5] F. Barbir, in: W. Vielstich, A. Lamm, H.A. Gasteiger (Eds.), Handbook of Fuel Cells, John Wiley & Sons Ltd., 2003, pp. 683–691 (Chapter 51).
[6] D.P. Wilkinson, J. St-Pierre, in: W. Vielstich, A. Lamm, H.A. Gasteiger (Eds.), Handbook of Fuel Cells, vol. 3, John Wiley & Sons Ltd., 2003, pp. 611–626 (Chapter 47).
[7] A.B. LaConti, M. Hamdan amd, R.C. McDonald, in: W. Vielstich, A. Lamm, H.A. Gasteiger (Eds.), Handbook of Fuel Cells, vol. 3, John Wiley & Sons Ltd., 2003, pp. 647–662 (Chapter 49).
[8] R. Baldwin, M. Pham, A. Leonida, J. McElroy, T. Nalette, J. Power Sources 29 (1990) 399–412.
[9] A.B. LaConti, Introduction to SPE Technology, in: Proceedings of Oronzio de Nora Symposium: Chlorine Technology, Venice Lido, Italy, May 15–18, 1979.
[10] J. St-Pierre, N. Jia, J. New Mater. Electrochem. Syst. 5 (2002) 263–271.
[11] O. Yamazaki, M. Echigo, T. Tabata, Abstracts from Fuel Cell Seminar 2002, Palm Springs, CA, November, 2002, pp. 105–108.
[12] M. Hicks, D. Ylitalo, Abstracts from Fuel Cell Seminar 2003, Miami Beach, FL, November, 2003, pp. 97–99.
[13] S.J.C. Cleghorn, J.A. Kolde, Abstract from Fuel Cell Seminar 2003, Miami Beach, FL, November, 2003, pp. 832–835.
[14] M. Takahashi, N. Kusunose, M. Aoki, A. Seya, Abstracts from Fuel Cell Seminar 2002, Palm Springs, CA, November, 2002, pp. 74–77.
[15] S.D. Knight, K.M. Colbow, J. St-Pierre, D. Wilkinson, J. Power Sources 127 (2004) 127–134.
[16] S.S. Kocha, in: W. Vielstich, A. Lamm, H.A. Gasteiger (Eds.), Handbook of Fuel Cells, vol. 3, John Wiley & Sons Ltd., 2003, pp. 538–565 (Chapter 43).
[17] T.E. Springer, T.A. Zawodzinski, M.S. Wilson, S. Gottesfeld, Electrochem. Soc. 143 (2) (1996) 587.
[18] D.A. Blom, J.R. Dunlap, A. Nolan, L.F. Allarda, J. Electrochem. Soc. 150 (4) (2003) A414.
[19] M.S. Wilson, F.H. Garzon, K.E. Sickafus, S. Gottesfeld, J. Electrochem. Soc. 140 (1993) 2872.
[20] C. Huang, K.S. Tan, J. Lin, K.L. Tan, Chem. Phys. Lett. 371 (2003) 80–84.
[21] B. Mattsson, H. Ericson, L.M. Torrell, F. Sundholm, Electrochim. Acta 45 (2000) 1405–1408.
[22] M. Murthy, D. Moore, Electrochemical Society Proccedings, vol. (in press), in: M. Murthy, K. Ota, J. W. Van Zee, S.R. Narayan, E. S. Takeuchi (Eds), Fourth International Symposium on PEM Fuel Cells, Honolulu, HI, 2004.
[23] M. Murthy, Electrochemical Society Proceedings, vol. PV 2002-31, in: M. Murthy, T.F. Fuller, J.W. Van Zee, S. Gottesfeld (Eds.), Third International Symposium on PEM Fuel Cells, Salt Lake City, UT, 2002, p. 257.
[24] S.J.C. Cleghorn, Abstracts from Fuel Cell Seminar 2000, Portland, OR, November, 2002, pp. 35–39.
[25] T. Patterson, Fuel Cell Technology; Oportunities and Challenges proceeding 2002 AIChE Spring National Meeting, New Orleans, LO, March, 2002, pp. 313–318.
[26] S.J.C. Cleghorn, J.A. Kolde, W. Liu, in: W. Vielstich, A. Lamm, H.A. Gasteiger (Eds.), Handbook of Fuel Cells, vol. 3, John Wiley & Sons Ltd., 2003, pp. 566–575 (Chapter 44).